Articles

A new approach of CeO_2 and La_2O_3 effects on the three-way catalysts containing low precious metals

WANG, Wen-Dong(汪文栋) LIN, Pei-Yan*(林培琰) FU, Yi-Lu(伏义路)
YU, Shou-Ming(俞寿明) MENG, Ming(孟明) ZHANG, Xiao-Peng(张霄鹏)
Department of Chemical Physics, University of Science and Technology of China, Hefei, Anhui 230026, China

A series of three-way catalysts (TWCs), containing a small amount of precious metals (PMs, including Pt, Pd and Rh) and a large amount of promoters CeO_2 and La_2O_3, were prepared with different precursor compounds and various doped manners. Crystal phases, dispersion of cerium and lanthanum, textural structure and thermal stability of the catalysts were investigated by XRD, XPS and pore parameters determination. The catalytic performance was studied by the measurements of CO, C_3H_6 and NO conversions on dependence of temperature at stoichimetric number point ($S = 1.00$), and from $S = 0.75$ to 1.30 at 280℃ or 340℃ for fresh or aged samples, respectively. The correlation between the catalytic performance and the characteristics of fresh and aged samples were discussed. The results show that the sample, in which CeO_2 and La_2O_3 are doped with mixed oxide powders, possesses poor dispersion and less thermal stability, and the conversions of NO and C_3H_6 are apparently lower than those of the samples aged at 850℃. The main reason is due to the lanthanum enrichment on the surface. The precious metals and cerium may be covered and enveloped, and the PMs located on the internal microporous surface where no cerium and lanthanum exist, are easier to sinter and oxidize. For the sample doped with $La(NO_3)_3$ and $Ce(NO_3)_3$ aqueous solutions, high dispersion and thermal stable CeO_2-La_2O_3 solid solution on all the surface of microporous γ-Al_2O_3 is identified. The solid solution CeO_2-La_2O_3 also possessed high dispersion in the sample doped with La_2O_3 powder and $Ce(NO_3)_3$ aqueous solution. The last two aged samples keep higher NO conversion at $S \geq 1$ region.

Keywords Doped manners, cerium oxide, lanthanum oxide, three-way catalyst, low precious metals

Introduction

Across the world, the motor vehicle is an indispensable part of today's modern society. There is now a fast developing market of automobiles in China. It is expected that the motor vehicle fleet will reach approximately 20 million by the year of 2000. However, the pollution caused by vehicle exhausts is so serious that there is much degradation of the air quality in most of the metropolises and cities. Therefore, substantial progresses should be made in reducing vehicles' emissions by the installation of catalytic converters. This would also meet the more stringent requirements of the forthcoming emission legislation. The cost of the catalyst mainly depends on the precious metals' content. However, it could be reduced by improving catalytic formulation and preparation techniques. Greatly reducing the cost of the three-way catalysts is expected to win competition in China market.

Both La_2O_3 and CeO_2 are extensively added as promoters to the current TWCs. La_2O_3 is a very effective thermal stabilizer for keeping high dispersion of Pt, Rh and retarding phase transition of γ-Al_2O_3 to keep high surface area.[1,2] The La^{3+} ion could greatly block interactions between Rh and γ-Al_2O_3.[3] It has been reported that CeO_2 is a crucial addition to current TWCs. Several functions are attributed to this addition, namely, stabilization of PM dispersion and its alumina support;[4] promotion of water gas shift reaction and steam reforming reaction;[5] suppression to the strong rhodium-alumina interaction.[6] However, the primary function of ceria in auto-

* Received November 12, 1999; accepted April 20, 2000.
Project (No. 9712301) supported by Ford-China Research and Development Fund.

motive exhaust catalysts is to provide oxygen storage capacity (OSC) in order to allow the catalyst to operate over a wider range of air/fuel ratio.[7] A notable approach was adopted to increase the oxygen storage capacity in the CeO_2 lattice by incorporating lower valent ions such as the rare earth (La, Y, Pr, Nd, *etc.*) and the alkaline earth (Ca, Sr, *etc.*),[8,9] which can create a corresponding number of anion vacancies. The oxygen storage capacity of the PM supported on $CeO_2/La_2O_3/Al_2O_3$ is much greater than that of the PM supported on CeO_2/Al_2O_3.[10] The synergetic effect was found by applying the optimum amount of ceria and lanthanum[11,12] in the TWCs.

Moreover, the dispersion and location states of both CeO_2 and La_2O_3 on the sample surface also greatly affect the activity and durability of the TWCs. However, the work concerned with this view is seldom reported. In this paper, doping of CeO_2 and La_2O_3 with different raw materials and with various doping procedures to the γ-Al_2O_3 supports are examined. It results in various dispersions and phases of Ce and La on the TWCs surface. The correlation of the textural properties, the bulk and surface phases and the different dispersion states of cerium and lanthanum with the CO, C_3H_6 and NO conversions are studied.

Experimental

Catalyst preparation

The low PM loading catalysts were prepared by wet impregnation of γ-alumina support in pellets of 40—60 mesh. Both the promoters La_2O_3 and CeO_2 with 30 wt% were mixed with γ-Al_2O_3 as oxides powder or impregnated as nitrates aqueous solution on γ-Al_2O_3 before doping precious metals. The samples that were impregnated with nitrate aqueous solutions of the promoters, were in advance calcined at 300℃ for 2 h in air to decompose the nitrates before doping precious metals. Co-impregnation of the precious metal salts $H_2PtCl_6 \cdot 6H_2O$, $PdCl_2$ and $RhCl_3 \cdot 3H_2O$ aqueous solution was adopted for all the samples. The total PM loading is 0.40 wt% on γ-Al_2O_3, including Pt 0.15 wt%, Pd 0.20 wt% and Rh 0.05 wt%. After co-impregnation, the precursors were dried at 120℃ for 4 h, and then calcined in air at 500℃ for 2 h. Fresh samples were reduced under hydrogen at 450℃ for 1 h.

The denotation of these samples, according to their different doped manners of the promoters, is listed in Table 1.

Table 1 Denotation of the samples

Catalyst	Doping form of cerium[a]	Doping form of lanthanum[a]
PM/Ce,La	M	M
PM-Ce/La[b]	I	M
PM-La/Ce[b]	M	I
PM-Ce-La[c]	I	I

[a] M: mixed with oxide powder; I: impregnated in nitrate aqueous solution. [b] Mixed with La_2O_3 (CeO_2) powder prior to being impregnated in cerium (lanthanum) nitrate aqueous solution. [c] Co-impregnated in cerium and lanthanum nitrate aqueous solution.

X-ray diffraction (XRD) *measurement*

XRD patterns were recorded on a D/MAX-γA rotatory target diffractometer, using Cu K_α (λ = 0.15418 nm) as X-ray source, operated at 40 KV and 100 mA.

X-ray photoelectron spectrum (XPS) *measurement*

The XPS data were obtained on an ESCALab MK2 spectrometer using Al K_α radiation. The XPS binding energies were referenced to the adventitious C_{1s} level at 284.6 eV.

Textural properties determination

The determination of surface area and pore volume was performed on an ASAP-2000 type surface and pore analyzer.

Catalytic test procedure

Light-off temperature

A simulated gas mixture (for example, CO 1.50 vol%, NO 1000 ppm, C_3H_6 1500 ppm and O_2 1.38 vol% with N_2 balanced) was used in this test. The composition of the reactant mixture was remained constant throughout the catalytic test at $S = 1.00$, where the stoichimetric number S is defined as $S = \{2[O_2] + [NO]\}/\{[CO] + 9[C_3H_6]\}$. When S is equal to uni-

ty, the oxidizing and reducing reactants are stoichimetric, and the conversions of CO, C_3H_6 and NO can simultaneously reach their theoretical maximum value. The results of this test are given in terms of light-off temperature, at which 50% of the reactant has been converted.

Conversions with various S values at constant temperature

In this test, the content of oxygen in the reactant mixture altered, so that the S values changed from 0.75 to 1.30, while the reaction temperature kept constant at 280℃ and 340℃ for fresh or aged sample, respectively.

Results

XRD *analysis*

The X-ray diffraction patterns of the fresh samples are shown in Fig. 1(A). The La_2O_3 peaks (d = 0.3270, 0.2003, 0.2832 nm) only appear for the sample PM/Ce,La, while the CeO_2 (d = 0.3124, 0.1913, 0.1632 nm) can be detected for all the four fresh samples. However, sharp CeO_2 peaks are observed for the PM-La/Ce and PM/Ce,La samples, in which the CeO_2 doped with oxide powder shows poor dispersion on the surface. For the other two samples, PM-Ce/La and PM-Ce-La, broaden CeO_2 peaks are revealed, which are attributed to the doped manner with cerium nitrate aqueous solution. The La_2O_3 is not detected for the sample PM-Ce/La, in which only the cerium is doped with nitrate aqueous solution. It implicates that impregnating of cerium nitrate aqueous solution can enhance the dispersion of original La_2O_3 oxide on the surface. Otherwise, the lanthanum doped with nitrate aqueous solution only results in the high dispersion of La_2O_3 itself in the sample PM-La/Ce. The reason may be that the cerium nitrate aqueous solution reacts with La_2O_3, and then a high-dispersed La^{3+} is formed. However, the lanthanum nitrate aqueous solution can not react with CeO_2 to form any Ce^{4+} or Ce^{3+}.

The lattice constants of CeO_2 with the different doped manners of La_2O_3 and CeO_2, estimated from the diffraction peak of $2\theta = 56.38°$ assigned to $CeO_2(311)$, are shown in Table 2. The larger lattice constants of CeO_2 are revealed for the samples PM-Ce-La and PM-Ce/La. It may be the dissolution of La^{3+} ions into the

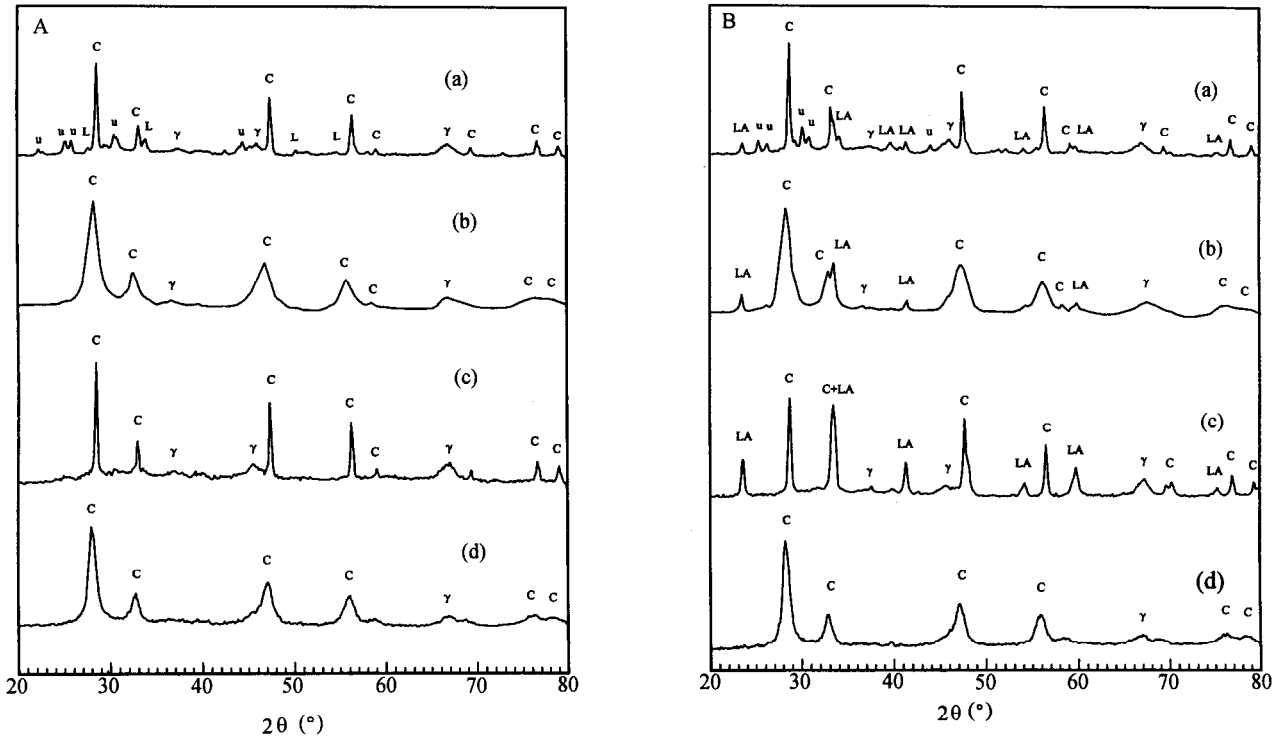

Fig. 1 XRD patterns of the fresh (A) and aged (B) samples with different CeO_2 and La_2O_3 doped manners. (a) PM/Ce,La; (b) PM-Ce/La; (c) PM-La/Ce; (d) PM-Ce-La; C: CeO_2; L: La_2O_3; LA: $LaAlO_3$; γ: γ-Al_2O_3; u: unknown.

CeO_2 lattice, since the radius of La^{3+} ion (0.119 nm) is larger than that of the Ce^{4+} ion (0.109 nm).[13] For the sample PM - Ce - La , the lattice constant of CeO_2 (0.5459 nm) is just equal to the calculated one (0.5459 nm), according to the linear relation between the lanthana content ($La_2O_3/(La_2O_3 + CeO_2)$) and the lattice constant of CeO_2-La_2O_3 solid solution.[10] Another identification is that the $LaAlO_3$ is not detected by XRD (Fig. 1(B)) for the sample PM-La-Ce after aging at 850℃, while the $LaAlO_3$ ($d = 0.2657$, 0.3800, 0.2188 nm) is found for the other three aged samples. Therefore, it makes sure that most of the La_2O_3, doped with nitrate aqueous solution, dissolved into the CeO_2 lattice. It is also noticed that the lattice constant of CeO_2 for the sample PM-Ce/La is larger than that of the pure CeO_2 to a certain extent. It implicates that the CeO_2-La_2O_3 solid solution is formed, although part of the La_2O_3 also remains. As mentioned above, the La^{3+} ions may be formed by the reaction between cerium nitrate aqueous solution and La_2O_3, and then the La^{3+} ions dissolve into the CeO_2 lattice in the calcination procedure at 500℃. The lattice constants of CeO_2 for the samples PM-La/Ce and PM/Ce,La, in which the CeO_2 is doped with oxide powder, are coincident with that of the pure CeO_2 (0.5412 nm). It means no dissolution of La^{3+} ions into the CeO_2 lattice.

Table 2 Estimation of CeO_2 lattice constant from XRD

Catalyst	2θ (°)	CeO_2 lattice constant[a] (nm)
pure CeO_2	56.38	0.5412
PM/Ce,La	56.38	0.5412
PM-La/Ce	56.39	0.5411
PM-Ce/La	56.04	0.5442
PM-Ce-La	55.86	0.5459

[a]Estimated from the diffraction peak of $2\theta = 56.38°$ assigned to CeO_2(311).

XPS *characterization*

X-ray photoelectron spectroscopy measurement was carried out for all the four fresh samples as well as the aged ones, in which XPS spectra of Ce_{3d} and La_{3d} are given in Figs. 2, 3, respectively. Larger granular CeO_2 in the samples may result in smaller ratio of Ce(surface)/Ce(bulk). Therefore, the relative intensity of binding energies (BE) assigned to Ce_{3d} is very weak for the sample PM/Ce,La, and even it is too weak to be

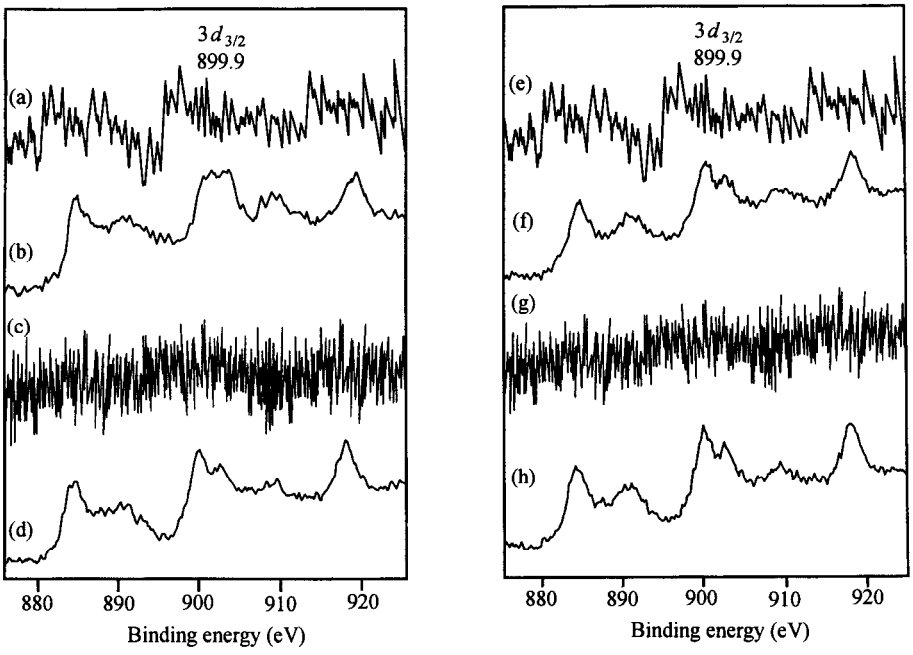

Fig. 2 XPS spectra of Ce_{3d}. (a)—(d): fresh samples; (e)—(h) aged samples; (a) & (e): PM/Ce,La; (b) & (f): PM-Ce/La; (c) & (g): PM-La/Ce; (d) & (h): PM-Ce-La.

detected for the sample PM-La/Ce. The binding energies assigned to Ce_{3d} for all the samples are the same as those for the pure CeO_2. Some investigations were carried out about the interaction between CeO_2 and Al_2O_3 to form $CeAlO_3$ precursor. The interaction occurred after reduction at 920℃ under H_2 atmosphere, and the formation of $CeAlO_3$ from CeO_2/Al_2O_3 was enhanced in the presence of Pd[14] and Pt[15]; during the reverse oxidation reaction at 500℃, the $CeAlO_3/Al_2O_3$ facilitated to CeO_2/Al_2O_3. However, there is no formation of $CeAlO_3$ precursor in this work according to the preparing conditions.

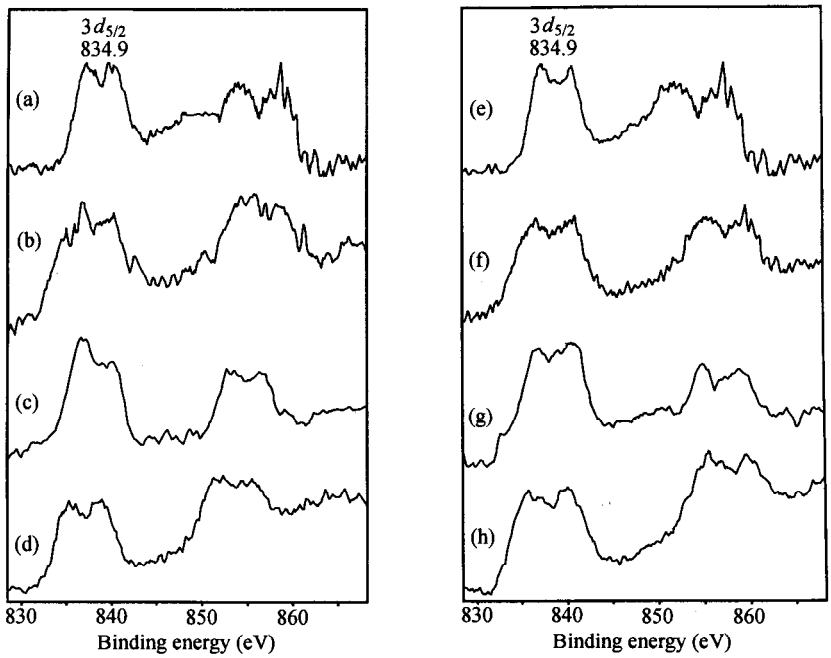

Fig. 3 XPS spectra of La_{3d}. (a)—(d): fresh samples; (e)—(h) aged samples; (a) & (e): PM/Ce, La; (b) & (f): PM-Ce/La; (c) & (g): PM-La/Ce; (d) & (h): PM-Ce-La.

Besides, the La/Ce atomic ratio (Table 3) on the surface is estimated from the XPS spectra. The calculated bulk La/Ce ratio is 1.06 according to the doped amount. The enrichment of Ce is only found on the fresh sample PM-Ce/La, in which the La_2O_3 is mixed to the γ-Al_2O_3 prior to impregnation of ceria nitrate solution. Moreover, the La/Ce ratio is almost not changed after aging. It means that the thermal stability of Ce and La distribution states on surface is high. It is observed that the enrichment of La_2O_3 is on the surface for the other three samples. The La/Ce ratio (4.30) on the surface of fresh PM/Ce, La, is larger than that of the fresh PM-Ce-La (1.15) apparently due to the poor dispersion of CeO_2 for the former, which is coincident with the XRD results. Moreover, the La/Ce ratio is twice larger after aging for the sample PM/Ce, La. It reflects the trend that the segregation of La_2O_3 occurs on the PM/Ce, La surface after aging, while the segregation of La_2O_3 is not obvious on the aged PM-Ce-La surface. It shows that the PM/Ce, La is the most thermally unstable sample among all the samples.

Textural properties

The pore volume on dependence of pore diameter for the samples is shown in Fig. 4, and the main results concerned with BET area and pore volume are listed in Table 4. The BET area of the support γ-alumina is equal to 148 m^2/g. The BET areas of the four samples, due to their different doped manners of La_2O_3 and CeO_2, are found to decrease to various degrees. When the La_2O_3 is doped with oxide powder, the BET areas of the sample PM/Ce, La and PM-Ce/La retain 109 and 103 m^2/g, respectively. While the lanthanum doped with nitrate aqueous solution, the areas decrease to 63.8 and 58.8 m^2/g for the sample PM-La/Ce and PM-Ce-La.

Table 3 Summary of the XPS results of samples

Catalyst	BE (eV)		La/Ce
	$Ce_{3d_{3/2}}$	$La_{3d_{5/2}}$	Atomic ratio[b]
PM/Ce, La fresh	897.6	834.7	4.30
aged	898.5	834.7	8.52
PM-Ce/La fresh	899.4	835.9	0.78
aged	898.6	835.6	0.82
PM-La/Ce fresh	ns[a]	834.8	/
aged	ns[a]	834.9	/
PM-Ce-La fresh	897.6	834.2	1.15
aged	898.2	834.8	1.32
CeO_2[c]	899.9	/	/
La_2O_3[c]	/	834.9	/

[a] ns: No signal can be detected. [b] The calculated La/Ce atomic ratio is 1.06 according to the doped materials. [c] From "*Handbook of X-ray Photoelectron Spectroscopy*" by Wagner, C.D., *etc*. Published by Perkin-Elmer Corporation (1979).

Table 4 Textural properties of samples

Sample	BET surface area (m^2/g)	Pore volume (mL/g)
γ-Al_2O_3	148	0.42
PM/Ce, La	109	0.30
PM-Ce/La	103	0.24
PM-La/Ce	63.8	0.17
PM-Ce-La	58.8	0.16

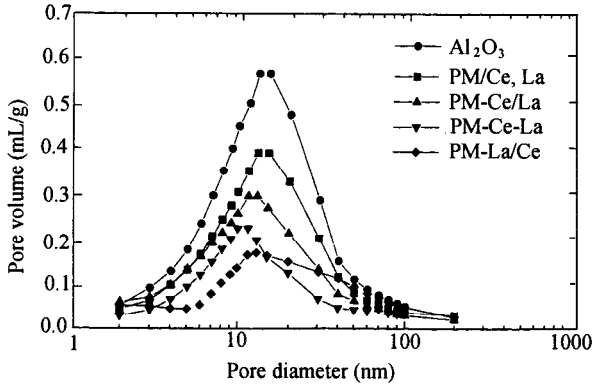

Fig. 4 Adsorption pore volume plot on dependence of pore diameter for γ-alumina and the samples.

It is shown that the pore volumes of the samples possess a similar alteration as the BET areas due to the different doped manners of La_2O_3 and CeO_2. The sequence of pore volume, as well as the BET surface area is γ-Al_2O_3 > PM/Ce, La > PM-Ce/La > > PM-La/Ce > PM-Ce-La.

Performances of three-way catalysts

The conversions of CO, C_3H_6 and NO dependence on temperature were measured under stoichimetric number $S = 1.00$ for all the fresh and aged samples. The light-off temperatures of CO, C_3H_6 and NO are obtained and listed in Table 5.

Table 5 Light-off temperature of CO, C_3H_6 and NO for granular catalysts[a]

Sample	Light-off temperature (℃)					
	Fresh sample[b]			Aged sample[c]		
	CO	C_3H_6	NO	CO	C_3H_6	NO
PM/Ce, La	228.1	238.0	236.6	298.4	317.8	320.5
PM-La/Ce	244.7	263.1	257.3	288.8	304.5	315.3
PM-Ce/La	268.0	282.9	275.6	284.2	323.7	290.4
PM-Ce-La	266.9	276.2	273.3	302.7	326.9	324.5

[a] Reaction conditions: sample of 600 mg, reactants of CO 1.5 vol%, C_3H_6 1500 ppm, NO 1000 ppm and O_2 1.00—1.75 vol%, balanced with N_2, SV (space velocity) = 9000 h^{-1}, reaction temperature is 280℃ and 340℃ for fresh and aged samples, respectively. [b] Fresh samples were pretreated in reactants effluent ($S = 1$) at 500℃, 0.5 h. *c* Aged samples were pretreated in atmosphere at 850℃, 2 h.

In Fig. 5(a)—(h) are shown the S traverse performance curves for all the fresh and aged samples at a constant reaction temperature 280℃ and 340℃, respectively. The conversions of CO, C_3H_6 and NO at S = 0.75, 1.00 and 1.30, as well as the width of S values at NO conversion ≥ 80% under oxidizing conditions ($S \geq 1.00$), are listed in Table 6.

Table 6 NO, CO and C_3H_6 conversion (%) at different S values[a]

Sample		Conversion (%)									W[b]
		$S=0.75$			$S=1.00$			$S=1.30$			
		NO	CO	C_3H_6	NO	CO	C_3H_6	NO	CO	C_3H_6	
PM/Ce, La	fresh[c]	94	100	48	98	100	92	43	100	100	0.05 (1.00—1.05)
	aged[d]	66	100	40	72	100	72	43	100	100	0
PM-La/Ce	fresh	92	100	50	92	100	96	52	100	100	0.10 (1.00—1.10)
	aged	51	67	43	72	100	97	36	100	99	0
PM-Ce/La	fresh	82	87	31	100	100	97	69	100	100	0.20 (1.00—1.20)
	aged	94	96	51	96	100	95	42	100	100	0.09 (1.00—1.09)
PM-Ce-La	fresh	74	80	36	100	100	98	60	100	100	0.06 (1.00—1.06)
	aged	93	100	48	100	100	97	54	100	100	0.04 (1.00—1.04)

[a] Reaction conditions: sample of 600 mg, reactants of CO 1.5 vol%, C_3H_6 1500 ppm, NO 1000 ppm and O_2 1.00—1.75 vol%, balanced with N_2, SV = 9000 h^{-1}, reaction temperature is 280℃ or 340℃ for fresh or aged sample, respectively. [b] Width of S values at the NO_x conversion ≥80% around $S \geq 1.00$. [c] Fresh samples were pretreated in reactants effluent ($S=1$) at 500℃, 0.5 h. [d] Aged samples were pretreated in atmosphere at 850℃, 2 h.

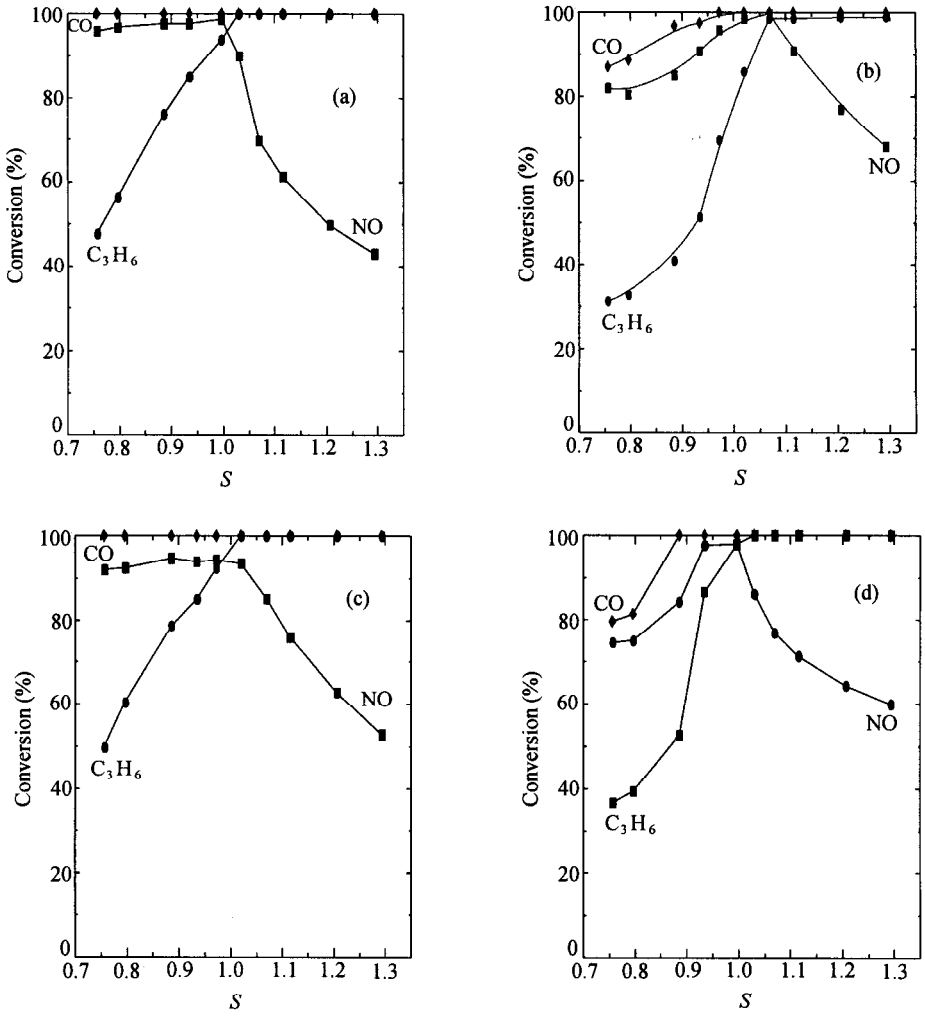

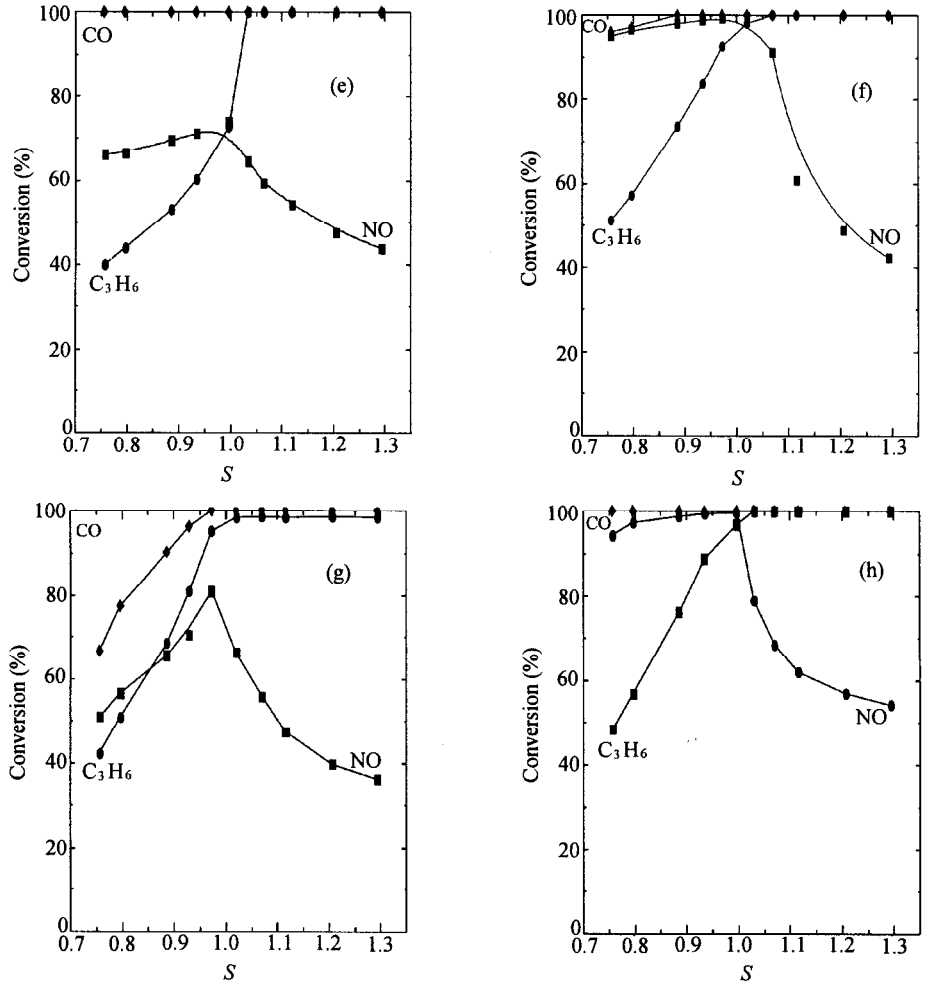

Fig. 5 Performance for granular three-way catalysts. (a)—(d): fresh catalysts pretreated in reactants atmosphere at 500℃ for 0.5 h. (e)—(h) catalysts aged in air at 850℃ for 2 h; (a) & (e): PM/Ce,La; (b) & (f): PM-Ce/La; (c) & (g): PM-La/Ce; (d) & (h): PM-Ce-La. Reaction conditions: samples of 600 mg, reactants of CO 1.5 vol%, C_3H_6 1500 ppm, NO 1000 ppm and O_2 1.00—1.75 vol%, balanced with N_2, reaction temperature is 280℃ and 340℃ for fresh and aged sample, respectively.

Discussions

Structure and textural differences for the samples

Based on results of XRD, XPS and textural properties characterizations, it is shown that there are great differences of the crystal phases, the location and dispersion states between cerium and lanthanum on the support γ-alumina surface because of their different doped manners. Poorly dispersed and discontinuous phases of cerium and lanthanum over the PM/Ce, La surface are revealed. The CeO_2 (~ 80 nm estimated from Scherrer equation) and La_2O_3 powder with larger particles size cannot mix with γ-alumina in molecular scale, and cannot enter its smaller pore either. Therefore, the BET surface and pore volume reduce slightly from those of γ-alumina. After aging at 850℃, severe enrichment of lanthanum on the surface is detected and $LaAlO_3$ crystal phase appears. In contrast, for the sample PM-Ce-La, the uniform mixed cerium and lanthanum nitrates aqueous solution can permeate to smaller pores with high dispersion on the entire surface. In this case, the well-dispersed solid solution of CeO_2-La_2O_3 is identified after calcination at 500℃ from XRD results, and therefore the BET surface and pore volume possess the smallest value among the four samples. Only slight enrichment of

lanthanum is found with high thermal stability and no $LaAlO_3$ is detected after aging at 850℃.

For the other two samples, PM-Ce/La and PM-La/Ce, the medium values of textural properties are shown, in that part of the larger particle size La_2O_3 for PM-Ce/La, and all the CeO_2 for PM-La/Ce may not enter to the smaller pores of γ-alumina internal surface. It is noticed that impregnating of the cerium nitrate aqueous solution enhances the dispersion of lanthanum on the sample PM-Ce/La. The formed La^{3+} solutes into CeO_2 lattice to form CeO_2-La_2O_3 solid solution during calcination at 500℃. After aging at 850℃, the rest part of La_2O_3, which may be the larger particle size La_2O_3, reacts with γ-alumina to form $LaAlO_3$. Otherwise, the dispersion of cerium on the PM-La/Ce can not enhance by impregnating of lanthanum nitrate aqueous solution. After aging at 850℃, only La is detected on the surface and Ce is not found on the sample PM-La/Ce surface. It means that the cerium may be embedded by lanthanum. Besides, the $LaAlO_3$ is formed obviously and no CeO_2-La_2O_3 solid solution exists after aging for this sample.

Correlation between the structure and the TWC *performance*

It is indicated that the fresh samples of PM/Ce, La and PM-La/Ce possess the higher CO, C_3H_6 and NO conversions in rich region at 280℃ and the lower light-off temperature at $S = 1.00$ than those of the other two samples. It was reported that large CeO_2 particles have more effective in generating active oxygen vacancy sites by a reducing treatment, which may result in a higher ability to activate molecules like CO,[16] CO_2[17] and NO[18] than that of the well-dispersed CeO_2 on PM-Ce/La and PM-Ce-La at rich region and at stoichimetric point. The oxygen vacancies associated with reduced ceria in proximity of PM particle have been suggested as active sites for NO and CO conversion.[19-21] The Pt, Pd and Rh active sites are kept high dispersion on all fresh samples surface.

After aging at atmosphere, the main factors to influence the CO, C_3H_6 oxidation and NO reduction, are the formation of the less active species PM-O on the surface, the agglomeration of PM particles, and Rh oxidation and diffusion into the γ-alumina lattice. Therefore, the CO, C_3H_6 and NO conversions decrease for all the samples to various extents, especially for the poor thermal stabilized aged samples PM/Ce, La and PM-La/Ce with enrichment of lanthanum on the surface. The PMs and cerium may be covered and enveloped by enriched lanthanum, and the PMs may sinter and be oxidized at the internal surface, on which no cerium or cerium and lanthanum locate as mentioned above. On the contrary, the aged samples PM-Ce/La and PM-Ce-La keep relative high conversions of NO at $S = 0.75$—1.00 region at 340℃. It may be attributed to the well dispersed and thermal stable solid solution CeO_2-La_2O_3 with enhanced oxygen storage capacity on the surface, which may also alleviate Rh sintering and oxidation, and alloy formation between PMs. It is also noticed that NO conversion on the fresh sample PM-Ce/La at lean region is relative higher and the window width of S value for NO conversion is wider than those of the other samples. These may be related to the intimate contact between the dispersed cerium and all the Rh sites. However, the NO conversion and window width reduce after aging. Therefore, it is critically important to improve the thermal stability of the cerium.

References

1. Huuska, M.; Maunula, T., *Proceeding of the 10th International Congress on Catalysis*, July, Budapest, Hungary, Elsevier Science Publishers B.V., 1992, p.2653.
2. Huang, Y.; Cant, N.M.; Guerbois, J.; Trimm, D.L.; Walpole, A., *Surf. Sci. Catal.*, **96**, 431(1995).
3. Usmen, R.K.; McCabe, R.W.; Haack, L.P.; Graham, G.W.; Hepburn, J.S.; Watkins, W.L.H., *J. Catal.*, **134**, 702(1992).
4. Gandhi, H.S.; Shelef, M., *Stud. Surf. Sci. Catal.*, **30**, 199(1987).
5. Kim, G., *Ind. Eng. Chem. Prod. Res. Dev.*, **21**, 267 (1982).
6. Harrison, B.; Diwell, A.F.; Hallett, C., *Plat. Met. Rev.*, 32(1988).
7. Yao, H.C.; Yao, Y.F., *J. Catal.*, **86**, 254(1984).
8. Nunan, J.G.; Cohn, M.J.; Donner, J.T., *Catal. Today*, **14**, 277(1992).
9. Bernal, S.; Blanco, G.; Cauqui, M.A.; Cifredo, G. A.; Pintado, J.M.; Rodriguez-Izquierdo, J.M., *Catal. Lett.*, **53**, 51(1998).
10. Miki, T.; Ogawa, T.; Haneda, M.; Kakuta, N.; Ueno, A.; Tateishi, S.; Matsuura, S.; Sato, M., *J. Phys. Chem.*, **94**, 6464(1990).
11. Nunan, J.G.; Williamson, W.B.; Robota, H.J., ASEC Manufacturing, SAE TECHNICAL PAPER SERIES, Society of Automotive Engineers, *PA, U. S. A. No. 960798*

(*1996*).
12. Lindner, D.; Lox, E.S.; Van Yperen, R.; Mufmann, L.; Kreuzer, T.P., *CATEC '97 Symposium*, Beijing, China, May, 1997.
13. *Kagaku-Binran*, *Kisohen II*, Ed. Japanese Chemical Society, Maruzen, Tokyo, 1984, p. II-717.
14. Shyu, J.Z.; Otto, K.; Watkins, W.L.H.; Graham, G. W.; Belitz, R.K.; Gandhi, H.S., *J. Catal.*, **114**, 23 (1988).
15. Shyu, J.Z.; Otto, K., *J. Catal.*, **115**, 16(1989).
16. Oh, S.H.; Eickel, C.C., *J. Catal.*, 112, 543(1988).
17. Trovarelli, A.; de Leitenberg, C.; Dolcetti, G.; Llorca, J., *J. Catal.*, **151**, 111(1995).
18. Cataluna, R.; Arcoya, A.; Seoane, X.L.; Martinez-Arias, A.; Coronado, L.M.; Conesa, J.C.; Soria, J.; Petrov, L.A., *Proc. III Int. Symp. CAPoC 3*, 1994, p. 89.
19. Oh, S.H., *J. Catal.*, **124**, 477(1990).
20. Loof, P.; Kasemo, B.; Bjornkvist, L; Andersson, S.; Frestad, A., *Stud. Surf. Sci. Catal.*, **71**, 253(1991).
21. Serre, C.; Garin, F.; Belot, G.;. Maire, G., *Stud. Surf. Sci. Catal.*, **141**, 9(1993).

(E9911156 SONG, J.P.; LING, J.)